

Article

# Green Synthesis of Silver Nanoparticles Using Bilberry and Red Currant Waste Extracts

Antonio Zuorro , Annalaura Iannone, Stefano Natali and Roberto Lavecchia \*

Department of Chemical Engineering, Materials and Environment, Sapienza University, 00184 Rome, Italy; antonio.zuorro@uniroma1.it (A.Z.); annalaura.iannone@uniroma1.it (A.I.); stefano.natali@uniroma1.it (S.N.)

\* Correspondence: roberto.lavecchia@uniroma1.it; Tel.: +39-06-44585598

Received: 19 March 2019; Accepted: 29 March 2019; Published: 3 April 2019



**Abstract:** The production of silver nanoparticles (Ag-NPs) from bilberry waste (BW) and red currant waste (RCW) extracts was studied. Red fruit extracts were obtained by treating BW and RCW with aqueous ethanol (50% *v/v*) at 40 °C. The formation of nanoparticles was monitored spectrophotometrically by measuring the intensity of the surface plasmon resonance band (SPR) of silver. The effects of temperature (20–60 °C) and pH (8–12) on the reaction kinetics and on the properties of Ag-NPs were investigated. Characterization by XRD and dynamic light scattering (DLS) techniques showed that Ag-NPs were highly crystalline, with a face-centered cubic structure and a hydrodynamic diameter of 25–65 nm. The zeta potential was in the range of −35.6 to −20.5 mV. Nanoparticles obtained from BW were slightly smaller and more stable than those from RCW. A kinetic analysis by the initial-rate method showed that there was an optimum pH, around 11, for the production of Ag-NPs. Overall, the results obtained suggest that BW and RCW can be advantageously used as a source of reducing and stabilizing agents for the green synthesis of Ag-NPs.

**Keywords:** green synthesis; silver nanoparticles; bilberry; red currant; agro-industrial wastes

## 1. Introduction

In recent years, silver nanoparticles (Ag-NPs) have been the subject of intense research, especially in the biomedical field [1–3], due to their superior properties when compared to their bulk counterpart [4]. Current technologies for the synthesis of nanoparticles are mostly based on the use of hazardous chemicals as reducing and stabilizing agents. Although they are highly efficient in terms of nanoparticle production, their environmental impact is not negligible. Furthermore, costly purification steps may be necessary if the complete removal of residual chemicals is required. This has prompted efforts to develop alternative green routes for the synthesis of Ag-NPs, such as those based on non-toxic chemicals [5,6] or using biological sources such as bacteria, fungi and plants [6–9]. Among them, processes using plant extracts from leaves, roots, fruits or seeds seem to be particularly promising due to their simplicity, safety and low cost [10,11].

Recently, as a further step towards the development of greener and more sustainable processes, attempts have been made to replace plant parts with agro-industrial wastes. For example, a study on persimmon waste investigated the suitability of each of the waste fractions: The seeds, the peels and the calyces, for producing Ag-NPs [12]. All of them were capable of synthesizing the nanoparticles, although the kinetics of nanoparticle formation and the particle size were found to depend on the waste fraction used. Other studies on different wastes, such as citrus peels [13] and grape stalks [14], supported the suitability of agro-industrial wastes for such purposes, but also confirmed the fact that the type of waste plays a key role in determining the properties of the obtained nanoparticles. Overall, the use of agro-industrial wastes for the eco-friendly production of nanoparticles seems to be promising, but the relatively few studies on these materials make it difficult to draw definitive

conclusions. In particular, little is known about how the nature of the waste affects the size and shape of nanoparticles, and of the possibility to control them by an appropriate selection of the reaction conditions.

This study was aimed at assessing the suitability of bilberry and red currant wastes as a source of reducing and stabilizing agents for the production of Ag-NPs. These materials contain significant amounts of phenolic compounds and other substances with metal-reducing capacity [15–17], although they present some differences in their levels and profiles [18]. Accordingly, the first objective of this paper was to evaluate whether these differences could have an effect on the characteristics of the synthesized Ag-NPs. Furthermore, we were interested in evaluating the influence of temperature and pH on the reaction kinetics and the properties of the nanoparticles. Different analytical techniques including UV-Vis spectroscopy, X-ray diffraction (XRD) and dynamic light scattering (DLS) were used.

The results obtained strongly support the use of the two red fruit wastes as a starting material for the synthesis of small-sized and stable Ag-NPs.

## 2. Materials and Methods

### 2.1. Chemicals and Waste Material

Silver nitrate was purchased from Caelo (Hilden, Germany). Ethanol, sodium hydroxide, sodium carbonate, sodium acetate trihydrate and ferric chloride hexahydrate were obtained from Carlo Erba (Milano, Italy). Potassium persulfate, hydrochloric acid (37 wt%), DPPH [2,2-diphenyl-1-picrylhydrazyl] and the Folin-Ciocalteu reagent were from Sigma-Aldrich Co. (St. Louis, Mo, USA). ABTS [2,2'-azino-bis (3-ethylbenzothiazoline-6-sulphonic acid)] and TPTZ [2,4,6-tri(2-pyridyl)-s-triazine] were from Alfa Aesar Haverhill (Massachusetts, USA). All chemicals were of analytical grade and used without further purification. Demineralized water was used for the preparation of aqueous solutions.

Fresh bilberry and red currant fruits were purchased from a local market. Red fruit wastes were obtained by collecting the solid residue from a food processing centrifuge (Moulinex, Ecully, France) fed with the whole fruits.

### 2.2. Production of Fruit Waste Extracts

Phenolic extracts were obtained from the plant material according to the procedure reported in [19]. The extraction was carried out in batch under stirring at  $40 \pm 0.1$  °C. Aqueous ethanol (50% *v/v*) was used as solvent. The liquid-to-solid ratio was 10 mL/g, the extraction time was 2 h and the stirring rate was 400 rpm. On completion of extraction, the liquid was separated from the solid by filtration and centrifuged at 10,000 rpm for 10 min. The extract was stored at 4 °C until use.

### 2.3. Analytical Methods

The total moisture content of BW and RCW was determined by oven drying ( $T = 105$  °C) to constant weight.

Total phenolics were determined by the Folin-Ciocalteu method following the procedure described in [20]. The results were expressed as gallic acid equivalents using a calibration curve obtained with gallic acid standards.

The antioxidant activity was determined by the DPPH, ABTS and ferric reducing antioxidant power (FRAP) methods, according to the procedures reported by Maietta et al. [21]. The results were expressed as Trolox equivalents (FRAP) using a calibration curve obtained with Trolox standards.

The formation of Ag-NPs was monitored spectrophotometrically (Shimadzu UV-2700 instrument, Kyoto, Japan) by measuring the intensity of the surface plasmon resonance (SPR) band of silver at 410–450 nm.

For XRD measurements, an X'Pert PRO diffractometer (Philips, Eindhoven, The Netherlands) operated at 40 kV and 30 mA with Cu K $\alpha$  radiation ( $\lambda = 1.5406 \text{ \AA}$ ) was used. The  $2\theta$  angle was varied from  $20^\circ$  to  $80^\circ$ . The step size was  $0.04^\circ$  and the counting time was 20 s per step.

Hydrodynamic diameter (HD) and zeta-potential measurements were made by dynamic light scattering (DLS) on a Litesizer<sup>TM</sup> 500 (Anton Paar, Graz, Austria).

#### 2.4. Synthesis of Ag-NPs

Ag-NPs were synthesized in thermostated and screw-capped glass vials equipped with a magnetic bar. The overall reaction volume was 10 mL and the two mixture components, the phenolic extract and the silver nitrate solution (3 mM) were added in amounts such as to obtain a silver-to-polyphenol ratio of 10 mol Ag<sup>+</sup>/mol GAE. The stirring rate was 350 rpm. At the desired time, a sample of the liquid was taken and assayed. The reaction temperature was varied between 20 and 60 °C, and the pH between 8 and 12 by appropriate additions of NaOH.

#### 2.5. Statistical Analysis

All synthesis reactions were performed in duplicate, while analytical determinations were repeated at least three times. The results were expressed as mean  $\pm$  standard deviation. Statistical analysis was carried out using Excel<sup>®</sup> data analysis software.

### 3. Results

#### 3.1. Characterization of Fruit Waste Extracts

The initial moisture contents of bilberry waste (BW) and red currant waste (RCW) were 78.6 and 76.5 wt%, respectively. The phenolic content of the waste extracts was  $3.47 \pm 0.1$  mmol GAE/L for BW and  $3.28 \pm 0.1$  mmol GAE/L for RCW. The antioxidant activities determined by the DPPH, ABTS and FRAP methods, expressed as Trolox equivalents, are reported in Figure 1. As commonly observed, the antioxidant activity values determined by the three assays were different, which can be explained by the fact that these methods involve different radical species and/or rely on different reactions. However, independent of the method used, the antioxidant capacity of BW extracts was higher than that of RCW extracts, paralleling the respective amounts of phenolic compounds.

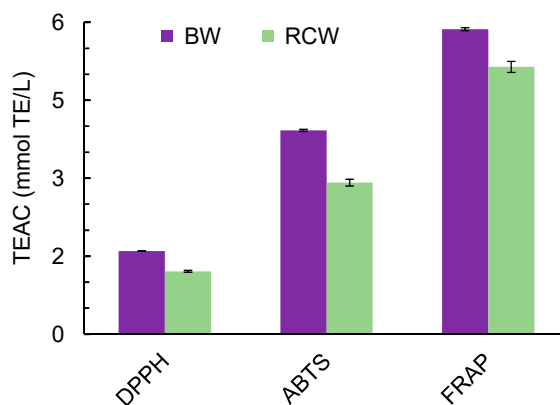


**Figure 1.** Trolox equivalent antioxidant capacity (TEAC) of bilberry waste (BW) and red currant waste (RCW) by the DPPH, ABTS and ferric reducing antioxidant power (FRAP) assays.

#### 3.2. Spectrophotometric Characterization of Ag-NPs

Typical UV-Vis spectra of reaction mixtures containing silver nitrate and BW or RCW extracts at fixed temperature and pH, and different reaction times are displayed in Figure 2. The presence of the strong SPR band at about 420 nm provides a clear indication of the production of Ag-NPs. For both

systems, this band appeared after about 15 min from the start of the reaction and its intensity increased with time up to about 5 h, when the reaction was complete.

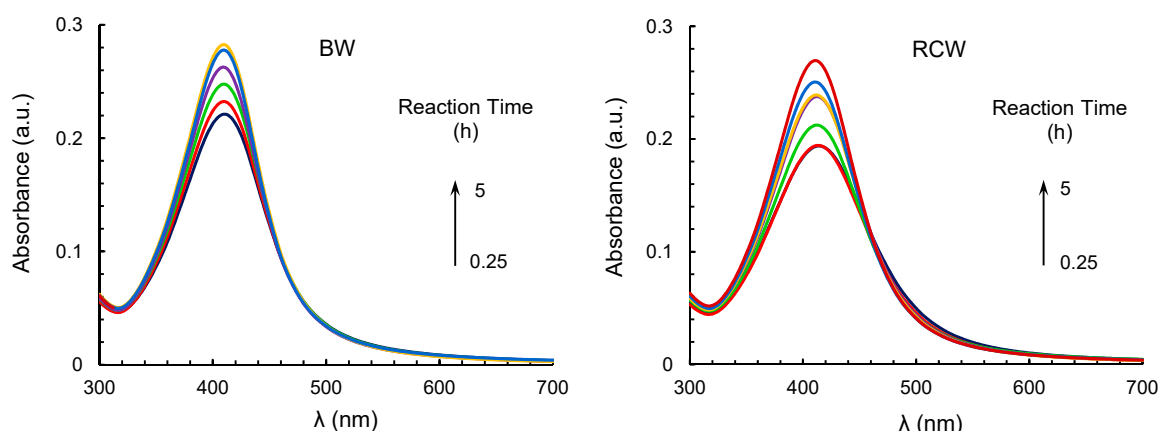


**Figure 2.** Spectrophotometric monitoring of the formation of silver nanoparticles (Ag-NPs) in reaction media containing silver nitrate and bilberry waste (BW) or red currant waste (RCW).

The formation of Ag-NPs was accompanied by a progressive color change of the solution from pale yellow to dark brown, which can be attributed to the excitation of surface plasmon vibrations in the nanoparticles [22]. The observed increase in the intensity of the SPR band is a reflection of the increase in the concentration of nanoparticles and therefore in the number of Ag-NPs produced.

The spectral position of the SPR band was affected by the reaction pH and temperature. An increase in pH from 8 to 12 caused a blue-shift of the band, which moved from 415 to 402 nm in systems containing BW extracts, and from 424 to 404 nm when RCW extracts were used (Figure 3). These spectral changes can be ascribed to a decrease in the size of metal nanoparticles, with alkaline conditions resulting in a smaller size of the synthesized Ag-NPs. In contrast, changing the temperature from 20 to 60 °C had minor effect on the spectral position of the SPR band (Figure 4).

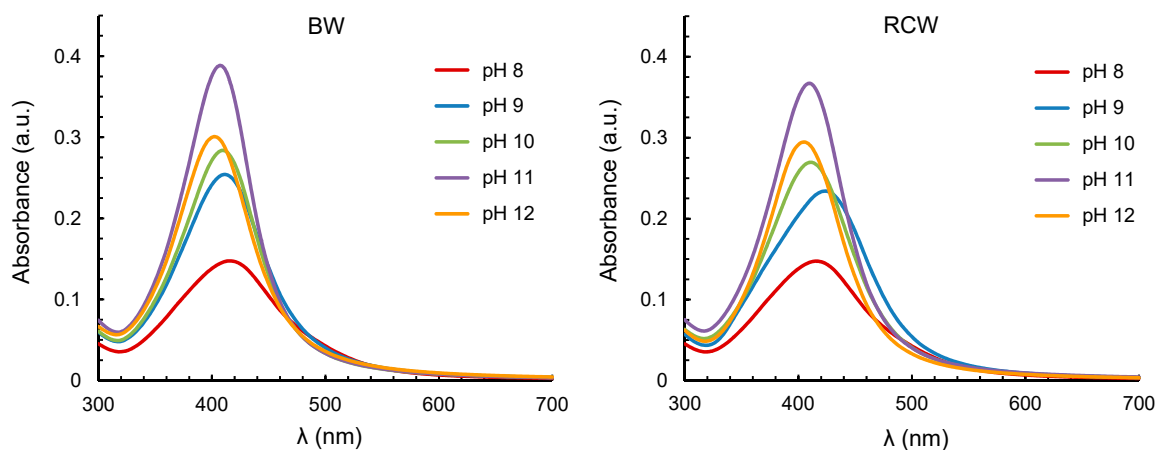


**Figure 3.** Effect of pH on the surface plasmon resonance (SPR) band of Ag-NPs obtained from bilberry waste (BW) and red currant waste (RCW) extracts (other conditions: T = 40 °C; Reaction time = 5 h; Silver-to-polyphenol ratio = 10 mol Ag<sup>+</sup>/mol GAE).

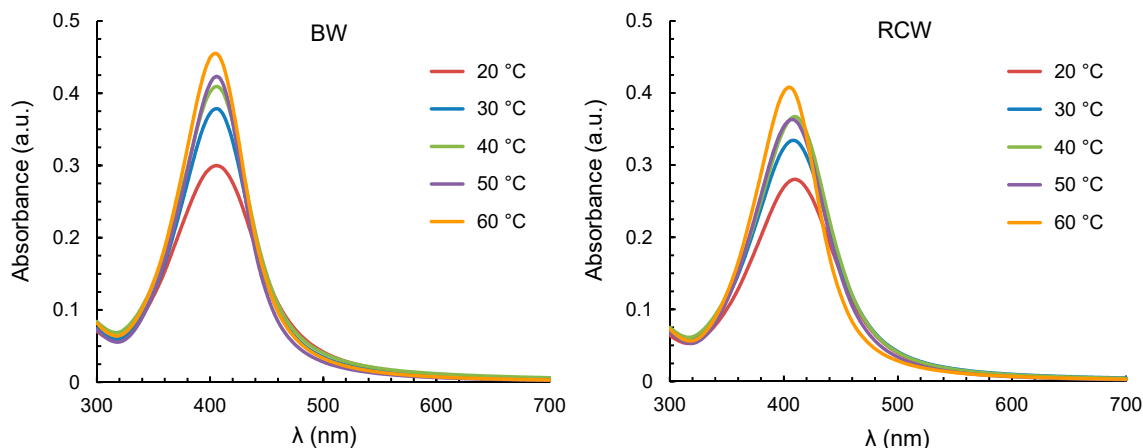


**Figure 4.** Effect of temperature on the SPR band of Ag-NPs obtained from bilberry waste (BW) and red currant waste (RCW) (other conditions: pH = 11; Reaction time = 5 h; Silver-to-polyphenol ratio = 10 mol Ag<sup>+</sup> / mol GAE).

The kinetics of nanoparticle formation was investigated by analyzing the time variation of the intensity of the SPR band. The analysis was performed by the initial-rate method. The experimental data at short times ( $t \leq 1$  h) were first smoothed using the following equation:

$$I_{max} = \frac{at}{b + t}, \quad (1)$$

where  $I_{max}$  is the intensity of the SPR band at  $\lambda_{max}$ . The parameters  $a$  and  $b$  were estimated by minimization of the sum of squared difference between experimental and calculated  $I_{max}$  values.

The initial rate of nanoparticle formation ( $r_0$ ) was then calculated from the slope of the tangent to the curve at  $t = 0$ :

$$r_0 = \left( \frac{dI_{max}}{dt} \right)_{t=0}, \quad (2)$$

which gives:

$$r_0 = \frac{b}{a}, \quad (3)$$

The estimated initial rates at different temperature and pH conditions are displayed in Figure 5. It can be seen that, at constant temperature and for both systems, the rate of nanoparticle formation was maximum at pH 11 (Figure 5a). At this pH, the reaction rate increased continuously with temperature (Figure 5b).

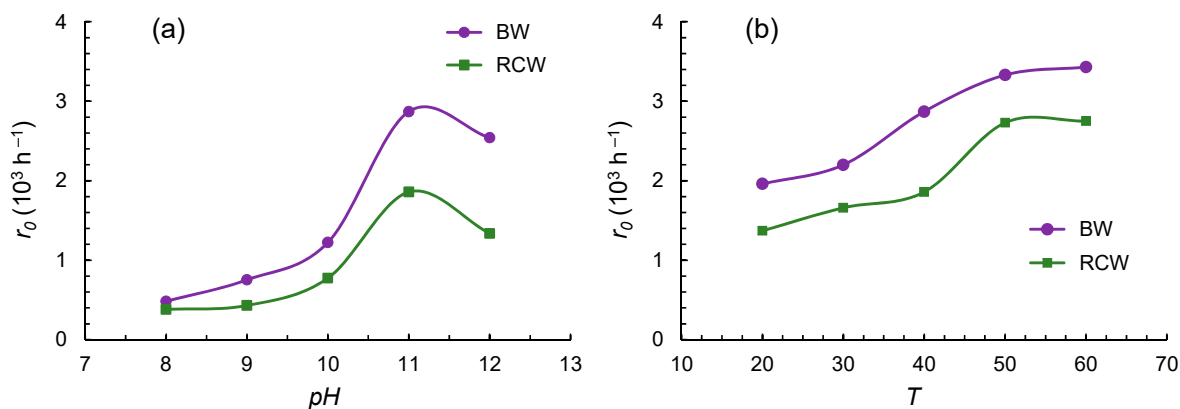


**Figure 5.** Effect of: (a) pH at  $T = 40$  °C and (b) temperature at pH = 11 on the initial rates ( $r_0$ ) of nanoparticle production from bilberry waste (BW) and red currant waste (RCW) extracts.

### 3.3. Characterization of Ag-NPs by DLS, Zeta Potential and XRD

Typical DLS size distribution profiles are shown in Figure 6. From these measurements, the HDs of the nanoparticles produced under different temperature and pH conditions were determined (Tables 1 and 2). In the same tables, the corresponding values of zeta potential are listed. As apparent, changing the reaction conditions resulted in the production of Ag-NPs of different size and stability.

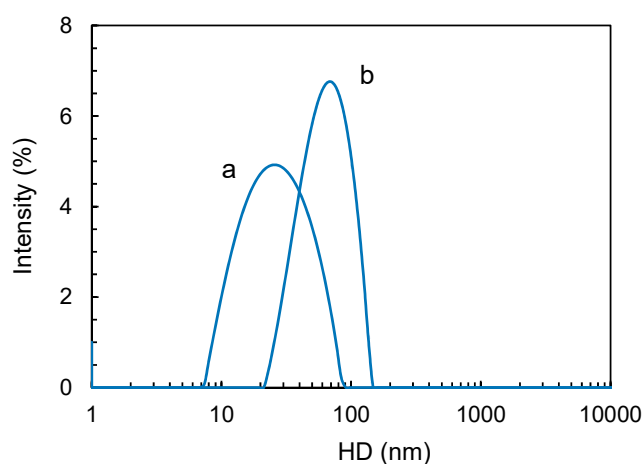


**Figure 6.** Dynamic light scattering (DLS) size distribution profiles of Ag-NPs obtained from red currant waste (RCW) extracts at 40 °C and pH 12 (a) or pH 9 (b) (other conditions: Reaction time = 5 h; Silver-to-polyphenol ratio = 10 mol Ag<sup>+</sup>/mol GAE).

**Table 1.** Hydrodynamic diameter (HD) and zeta potential ( $\zeta$ ) of Ag-NPs obtained from bilberry waste (BW) and red currant waste (RCW) extracts at different pH (other conditions: T = 40 °C; Reaction time = 5 h; Silver-to-polyphenol ratio = 10 mol Ag<sup>+</sup>/mol GAE).

pH	HD (nm)		$\zeta$ (mV)	
	BW	RCW	BW	RCW
8	45.3 ± 0.1	49.5 ± 1.2	−23.4 ± 1.0	−25.5 ± 1.3
9	50.8 ± 1.0	55.5 ± 2.0	−28.7 ± 1.4	−22.0 ± 1.1
10	47.7 ± 0.9	56.9 ± 0.5	−20.5 ± 0.8	−28.4 ± 1.0
11	37.7 ± 1.4	43.8 ± 0.4	−35.6 ± 1.1	−25.5 ± 1.5
12	29.4 ± 0.5	25.4 ± 1.4	−31.6 ± 1.2	−26.6 ± 0.9

**Table 2.** Hydrodynamic diameter (HD) and zeta potential ( $\zeta$ ) of Ag-NPs obtained from bilberry waste (BW) and red currant waste (RCW) extracts at different temperatures (other conditions: pH = 11; Reaction time = 5 h; Silver-to-polyphenol ratio = 10 mol Ag<sup>+</sup>/mol GAE).

T (°C)	HD (nm)		$\zeta$ (mV)	
	BW	RCW	BW	RCW
20	63.1 ± 0.6	64.6 ± 0.8	−28.8 ± 1.1	−29.0 ± 0.9
30	53.9 ± 2.5	51.1 ± 2.7	−27.3 ± 1.4	−27.5 ± 0.8
40	37.7 ± 1.4	43.8 ± 0.4	−35.6 ± 1.1	−25.5 ± 1.5
50	41.7 ± 0.4	44.7 ± 0.4	−25.0 ± 0.6	−24.9 ± 1.2
60	36.7 ± 2.2	43.4 ± 0.8	−31.6 ± 1.2	−26.6 ± 0.9

HDs ranged from 25.4 to 64.6 nm, while zeta potential varied between −35.6 and −20.5 mV. XRD patterns of the Ag-NPs obtained from the two waste extracts are displayed in Figure 7. As can be seen, the synthesized nanoparticles exhibited a high crystallinity. In the 2 $\theta$  range of 20–80°, four intense peaks were observed, at about 38°, 44°, 64.5° and 77°. They correspond, respectively, to the planes (111), (200), (220) and (311) of the face-centered cubic structure of metallic silver. The peak at about 38° was the most intense, indicating that the preferred orientation was along the (111) plane.

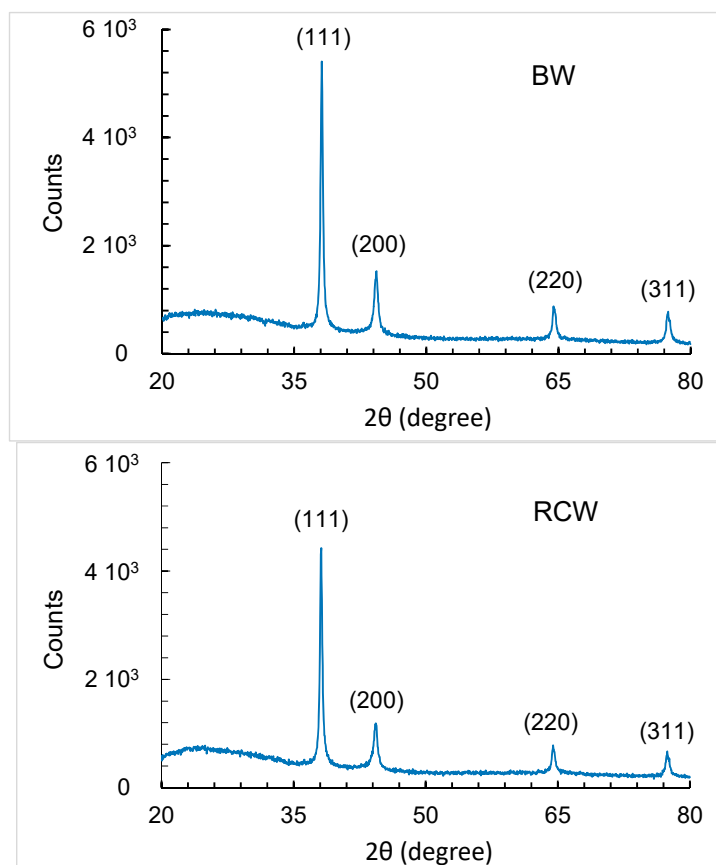


**Figure 7.** XRD patterns of Ag-NPs obtained from bilberry waste (BW) and red currant waste (RCW) extracts with the four peaks corresponding to metallic silver.

#### 4. Discussion

The use of plant extracts for the synthesis of metal nanoparticles has attracted increasing interest in the last years due to its advantages over traditional chemical methods as well as over the utilization of bacteria, fungi or other living organisms. A review of the literature shows that the production of nanoparticles by this approach is easy, fast and cost-effective [23,24]. Recently, agro-industrial wastes have been investigated as potential starting materials for the green synthesis of nanoparticles [12–14,25]. However, there are still few reports in the literature that explore their suitability for such applications. Accordingly, this study was undertaken to determine whether Ag-NPs could be prepared using aqueous extracts from BW and RCW. Like other fruit wastes, BW and RCW are generated in large amounts by the fruit juice industry. They consist mainly of the fruit skins and seeds, which are known to contain phenolic compounds and other phytochemicals with antioxidant and metal-reducing properties [26].

Phenolic compounds are a class of low-molecular-weight secondary metabolites occurring ubiquitously in plants [27]. Because of their protective role against oxidative damage and antimicrobial agents, they are located mainly in the outer layers of plant tissues, which explains the high levels of phenolic compounds that are usually found in agro-industrial wastes. A comparative study on pomaces from various red fruits (blueberry, raspberry, red currant and blackberry) showed that all of them were important sources of phenolic compounds, although their amount and profile varied significantly with the waste type [17]. In most dark-colored berries, anthocyanins represent the major class of phenolics [18]. In bilberry, anthocyanins and flavonol glycosides are the only groups of phenolic compounds; while in red currant, hexoside derivatives of caffeic, coumaroylquinic and vanillic acids are the most abundant compounds [18].

The results presented here clearly indicate that aqueous extracts from BW and RCW are suitable materials for the green synthesis of Ag-NPs. In particular, the following points can be made: (1) nanoparticles obtained from BW are slightly smaller and more stable than those from RCW (Tables 1 and 2); (2) the kinetics of nanoparticle formation is affected by the pH and the temperature (Figures 3 and 4); and (3) according to initial-rate data, an optimum pH exists, around 11, while there does not seem to be an optimum temperature, at least in the temperature range studied (Figure 5).

The greater effectiveness of BW over RCW extracts can be attributed to their higher phenolic content and reducing capacity. As regards the mechanisms of nanoparticle formation in the presence of phenolic compounds, most of the current knowledge comes from studies on model compounds, particularly phenolic acids. Phenolic acids are characterized by the presence, in their molecular structure, of a carboxylic acid group and one or more hydroxyl groups, which confer antioxidant activity to them [28]. It is generally agreed that both the hydroxyl and the carboxylic acid groups are involved in the formation of nanoparticles [29–31]. In particular, the hydroxyl groups are responsible for the reduction of metal ions to the zero-valent metal, while the carboxyl groups act as stabilizing agents. In the case of gallic acid (GA), the formation of Ag-NPs proceeds through an electron transfer mechanism in which GA is oxidized to its quinone form (GAQ):



and silver ions are reduced to metallic silver:



From the aggregation of metal nuclei, primary nanoparticles are formed:



which grow up to a final size determined by the formation of a layer of GAQ molecules around the Ag-NPs [29]. In this capping layer, the carboxylic groups of GAQ interact with the surface of the metal nanoparticle and hydrogen bonds are formed between hydroxyl groups of adjacent GAQ molecules. Similar considerations can be made for other phenolic compounds, not necessarily having a carboxylic acid group and a dihydroxy moiety in their molecules. Nevertheless, the evidence so far indicates that the number of hydroxyl groups and their relative position on the aromatic ring may affect the formation and the characteristics of the metal nanoparticles [30,32]. In particular, a phenolic compound should have at least two hydroxyl groups at ortho or para positions on its molecule for the reaction to proceed.

The sharp and narrow SPR band observed under different pH and temperature conditions suggests that small-sized and monodisperse Ag-NPs are formed. The intensity of this band and the initial rate of nanoparticle formation increased with pH up to 11, above which value they tended to decrease. Similar results were obtained in studies on other plant wastes, such as *Cocos nucifera* coir [33] and sacha inchi (*Plukenetia volubilis* L.) shell biomass [34], where the production of Ag-NPs was found to be pH dependent, with an optimum pH close to 12.

The effect of pH can be explained by considering that the oxidation of phenolic compounds is accompanied by the release of  $\text{H}^+$  ions (Equation (1)) and hence, the nucleation of Ag-NPs is favored under alkaline conditions. As a result, at higher pH more small-sized nanoparticles are formed, which is also confirmed by the blue-shift of the SPR band and the measured HDs. However, high pH values may also favor the production of  $\text{Ag}_2\text{O}$ , according to the reaction [35]:



which could explain the observed decreases in the intensity of the SPR band and in the initial rates at pH 12. It should also be considered that the electrostatic interactions of the capping agents with

the surface of the nanoparticles, which control the formation and the strength of the capping layer, increase at acidic pH [29]. Therefore, the net effect of pH on the synthesis and properties of Ag-NPs will result from the contribution of each of these mechanisms.

Regarding the temperature, an increase from 20 to 60 °C resulted in a substantial increase of both the SPR band intensity and the initial rate of nanoparticle formation. This is a clear reflection of the positive effect of temperature on the kinetics of nanoparticle formation. An increase in temperature also resulted in a size reduction of Ag-NPs, indicating that, in the temperature range investigated, nucleation is favored over growth. A positive effect of temperature on the kinetics of nanoparticle formation is commonly observed [36–38]. Again, however, it should be pointed out that the temperature can affect the characteristics of the resulting nanoparticles in an unpredictable way, as this variable can have different effects on the steps of the overall synthesis process. So, in a study on the production of Ag-NPs using *Pinus eldarica* bark extract, an increase of the reaction temperature from 25 to 150 °C led to a progressive decrease in nanoparticle size [39]. Conversely, in another study using aqueous extracts of *Lippia citriodora* leaves, increasing the temperature from 25 to 95 °C enhanced the kinetics of nanoparticle formation but did not influence significantly the size of Ag-NPs [40].

## 5. Conclusions

The results of this study demonstrate that BW and RCW can be effectively used as a source of reducing and stabilizing agents for the synthesis of Ag-NPs. Under the investigated conditions, small-sized and stable nanoparticles were obtained. Furthermore, the kinetic analysis of the data provided indications of the influence of pH and temperature on the synthesis reaction.

Further research should be directed at evaluating the suitability of these wastes for the production of other types of nanoparticles. Due to the limited understanding of the underlying mechanisms, identification of the main bioactive compounds in these materials would be helpful in assessing their role in the formation and stabilization of the nanoparticles. Direct determination of the nanoparticle size and shape by Transmission Electron Microscopy (TEM) imaging and the possibility of controlling them by varying the reaction conditions are other interesting topics to be investigated in the future.

**Author Contributions:** Designed the experiments and analyzed the data and wrote the paper, A.Z.; Carried out the experiments, A.I.; Performed XRD measurements and analyzed the data, S.N.; Contributed to the design of experiments, interpreted the data and wrote the paper, R.L.

**Funding:** This research was partially supported by grants from Sapienza University of Rome (Italy).

**Acknowledgments:** The authors are grateful to Maria Gioia for her assistance in the experimental work.

**Conflicts of Interest:** The authors declare no conflict of interest.

## References

1. Verma, S.; Abirami, S.; Mahalakshmi, V. Anticancer and antibacterial activity of silver nanoparticles biosynthesized by *Penicillium* spp. and its synergistic effect with antibiotics. *J. Microbiol. Biotechnol. Res.* **2013**, *3*, 54–71.
2. Blanco, S.; Uribe, P.; Moreno, D.; Ortiz, C.C.; Gutiérrez, J. Self-assembled polymer layer with silver nanoparticles as an alternative coating for biomedical applications. *Chem. Eng. Trans.* **2018**, *64*, 631–636.
3. Deshmukh, S.P.; Patil, S.M.; Mullani, S.B.; Delekar, S.D. Silver nanoparticles as an effective disinfectant: A review. *Mater. Sci. Eng. C Mater. Biol. Appl.* **2019**, *97*, 954–965. [[CrossRef](#)]
4. Gangula, A.; Podila, R.; Ramakrishna, M.; Karanam, L.; Janardhana, C.; Rao, A.M. Catalytic reduction of 4-nitrophenol using biogenic gold and silver nanoparticles derived from *Breynia rhamnoides*. *Langmuir* **2011**, *27*, 15268–15274. [[CrossRef](#)]
5. Cheviron, P.; Gouanvé, F.; Espuche, E. Green synthesis of colloid silver nanoparticles and resulting biodegradable starch/silver nanocomposites. *Carbohydr. Polym.* **2014**, *108*, 291–298. [[CrossRef](#)] [[PubMed](#)]
6. Michna, A.; Morga, M.; Adamczyk, Z.; Kubiak, K. Monolayers of silver nanoparticles obtained by green synthesis on macrocation modified substrates. *Mater. Chem. Phys.* **2019**, *227*, 224–235. [[CrossRef](#)]

7. Marchiol, L.; Mattiello, A.; Pošćić, F.; Giordano, C.; Musetti, R. In vivo synthesis of nanomaterials in plants: Location of silver nanoparticles and plant metabolism. *Nanoscale Res. Lett.* **2014**, *9*, 101. [[CrossRef](#)] [[PubMed](#)]
8. Singh, R.; Shedbalkar, U.U.; Wadhvani, S.A.; Chopade, B.A. Bacteriogenic silver nanoparticles: Synthesis, mechanism, and applications. *Appl. Microbiol. Biotechnol.* **2015**, *99*, 4579–4593. [[CrossRef](#)] [[PubMed](#)]
9. Sonar, H.; Nagaonkar, D.; Ingle, A.P.; Rai, M. Mycosynthesized silver nanoparticles as potent growth inhibitory agents against selected waterborne human pathogens. *Clean–Soil Air Water* **2017**, *45*, 1600247. [[CrossRef](#)]
10. Sadeghi, B.; Gholamhoseinpoor, F. A study on the stability and green synthesis of silver nanoparticles using *Ziziphora tenuior* (Zt) extract at room temperature. *Spectroc. Acta Part A Molec. Biomolec. Spectr.* **2015**, *134*, 310–315. [[CrossRef](#)] [[PubMed](#)]
11. Mamatha, R.; Khan, S.; Salunkhe, P.; Satpute, S.; Kendurkar, S.; Prabhune, A.; Deval, A.; Chaudhari, B.P. Rapid synthesis of highly monodispersed silver nanoparticles from the leaves of *Salvadora persica*. *Mater. Lett.* **2017**, *205*, 226–229. [[CrossRef](#)]
12. Ramachandriah, K.; Gnoc, N.T.B.; Chin, K.B. Biosynthesis of silver nanoparticles from persimmon byproducts and incorporation in biodegradable sodium alginate thin film. *J. Food Sci.* **2017**, *82*, 2329–2336. [[CrossRef](#)]
13. Dauthal, P.; Mukhopadhyay, M. Agro-industrial waste-mediated synthesis and characterization of gold and silver nanoparticles and their catalytic activity for 4-nitroaniline hydrogenation. *Korean J. Chem. Eng.* **2015**, *32*, 837–844. [[CrossRef](#)]
14. Bastos-Arrieta, J.; Florido, A.; Pérez-Ràfols, C.; Serrano, N.; Fiol, N.; Poch, J.; Villaescusa, I. Green synthesis of Ag nanoparticles using grape stalk waste extract for the modification of screen-printed electrodes. *Nanomaterials* **2018**, *8*, 946. [[CrossRef](#)]
15. Fidaleo, M.; Lavecchia, R.; Zuorro, A. Extraction of bioactive polyphenols with high antioxidant activity from bilberry (*Vaccinium myrtillus* L.) processing waste. *Orient. J. Chem.* **2016**, *32*, 759–767. [[CrossRef](#)]
16. Tian, Y.; Liimatainen, J.; Alanne, A.-L.; Lindstedt, A.; Liu, P.; Sinkkonen, J.; Kallio, H.; Yang, B. Phenolic compounds extracted by acidic aqueous ethanol from berries and leaves of different berry plants. *Food Chem.* **2017**, *220*, 266–281. [[CrossRef](#)] [[PubMed](#)]
17. Jara-Palacios, M.J.; Santisteban, A.; Gordillo, B.; Hernanz, D.; Heredia, F.J.; Escudero-Gilete, M.L. Comparative study of red berry pomaces (blueberry, red raspberry, red currant and blackberry) as source of antioxidants and pigments. *Eur. Food Res. Technol.* **2019**, *245*, 1–9. [[CrossRef](#)]
18. Gavrilova, V.; Kajdžanoska, M.; Gjamovski, V.; Stefova, M. Separation, characterization and quantification of phenolic compounds in blueberries and red and black currants by HPLC-DAD-ESI-MSn. *J. Agric. Food Chem.* **2011**, *59*, 4009–4018. [[CrossRef](#)] [[PubMed](#)]
19. Zuorro, A. Optimization of polyphenol recovery from espresso coffee residues using factorial design and response surface methodology. *Sep. Purif. Technol.* **2015**, *152*, 64–69. [[CrossRef](#)]
20. Zuorro, A.; Lavecchia, R. Influence of extraction conditions on the recovery of phenolic antioxidants from spent coffee grounds. *Am. J. Appl. Sci.* **2013**, *10*, 478–486. [[CrossRef](#)]
21. Maietta, M.; Colombo, R.; Lavecchia, R.; Sorrenti, M.; Zuorro, A.; Papetti, A. Artichoke (*Cynara cardunculus* L. var. scolymus) waste as a natural source of carbonyl trapping and antiglycative agents. *Food Res. Int.* **2017**, *100*, 180–190. [[CrossRef](#)] [[PubMed](#)]
22. Dang, D.M.T.; Dang, C.M.; Fribourg-Blanc, E. Study of the formation of silver nanoparticles and silver nanoplates by chemical reduction method. *Int. J. Nanotechnol.* **2015**, *12*, 456–465. [[CrossRef](#)]
23. Khan, M.; Shaik, M.R.; Adil, S.F.; Khan, S.T.; Al-Warthan, A.; Siddiqui, M.R.H.; Tahir, M.N.; Tremel, W. Plant extracts as green reductants for the synthesis of silver nanoparticles: Lessons from chemical synthesis. *Dalton Trans.* **2018**, *47*, 11988–12010. [[CrossRef](#)] [[PubMed](#)]
24. Fahimirad, S.; Ajalloueiian, F.; Ghorbanpour, M. Synthesis and therapeutic potential of silver nanomaterials derived from plant extracts. *Ecotoxicol. Environ. Saf.* **2019**, *168*, 260–278. [[CrossRef](#)]
25. Kumar, R.; Roopan, S.M.; Prabhakarn, A.; Khanna, V.G.; Chakraborty, S. Agricultural waste *Annona squamosa* peel extract: Biosynthesis of silver nanoparticles. *Spectrochim. Acta Part A* **2012**, *90*, 173–176. [[CrossRef](#)]
26. de Camargo, A.C.; Schwember, A.R.; Parada, R.; Garcia, S.; Maróstica, M.R.; Franchin, M.; Regitano-d’Arce, M.A.B.; Shahidi, F. Opinion on the hurdles and potential health benefits in value-added use of plant food processing by-products as sources of phenolic compounds. *Int. J. Mol. Sci.* **2018**, *19*, 3498. [[CrossRef](#)]

27. Weber, F.; Passon, B. Characterization and Quantification of Polyphenols in Fruits. In *Polyphenols in Plants: Isolation, Purification and Extract Preparation*, 2nd ed.; Watson, R.R., Ed.; Academic Press: London, UK, 2018; pp. 111–121.
28. Bravo, L. Polyphenols: Chemistry, dietary sources, metabolism, and nutritional significance. *Nutr. Rev.* **1998**, *56*, 317–333. [[CrossRef](#)]
29. Yoosaf, K.; Ipe, B.I.; Suresh, C.H.; Thomas, K.G. In situ synthesis of metal nanoparticles and selective naked-eye detection of lead ions from aqueous media. *J. Phys. Chem. C* **2007**, *111*, 12839–12847. [[CrossRef](#)]
30. Bhutto, A.A.; Kalay, S.; Sherazi, S.T.H.; Culha, M. Quantitative structure–activity relationship between antioxidant capacity of phenolic compounds and the plasmonic properties of silver nanoparticles. *Talanta* **2018**, *189*, 174–181. [[CrossRef](#)] [[PubMed](#)]
31. Liu, Y.-S.; Chang, Y.-C.; Chen, H.-H. Silver nanoparticle biosynthesis by using phenolic acids in rice husk extract as reducing agents and dispersants. *J. Food Drug Anal.* **2018**, *26*, 649–656. [[CrossRef](#)]
32. Özyürek, M.; Güngör, N.; Baki, S.; Güçlü, K.; Apak, R. Development of a silver nanoparticle-based method for the antioxidant capacity measurement of polyphenols. *Anal. Chem.* **2012**, *84*, 8052–8059. [[CrossRef](#)] [[PubMed](#)]
33. Roopan, S.M.; Rohit; Madhumitha, G.; Rahuman, A.A.; Kamaraj, C.; Bharathi, A.; Surendra, T.V. Low-cost and eco-friendly phyto-synthesis of silver nanoparticles using *Cocos nucifera* coir extract and its larvicidal activity. *Ind. Crop. Prod.* **2013**, *43*, 631–635. [[CrossRef](#)]
34. Kumar, B.; Smita, K.; Cumbal, L.; Debut, A. Sacha inchi (*Plukenetia volubilis* L.) shell biomass for synthesis of silver nanocatalyst. *J. Saudi Chem. Soc.* **2017**, *21*, S293–S298. [[CrossRef](#)]
35. Adegboyega, N.F.; Sharma, V.K.; Siskova, K.; Zbořil, R.; Sohn, M.; Schultz, B.J.; Banerjee, S. Interactions of aqueous Ag<sup>+</sup> with fulvic acids: Mechanisms of silver nanoparticle formation and investigation of stability. *Environ. Sci. Technol.* **2013**, *47*, 757–764. [[CrossRef](#)] [[PubMed](#)]
36. Baghizadeh, A.; Ranjbar, S.; Gupta, V.K.; Asif, M.; Pourseyedi, S.; Karimi, M.J.; Mohammadinejad, R. Green synthesis of silver nanoparticles using seed extract of *Calendula officinalis* in liquid phase. *J. Mol. Liq.* **2015**, *207*, 159–163. [[CrossRef](#)]
37. Mashwani, Z.-U.-R.; Khan, T.; Khan, M.A.; Nadhman, A. Synthesis in plants and plant extracts of silver nanoparticles with potent antimicrobial properties: Current status and future prospects. *Appl. Microbiol. Biotechnol.* **2015**, *99*, 9923–9934. [[CrossRef](#)] [[PubMed](#)]
38. Yuan, C.-G.; Huo, C.; Gui, B.; Liu, P.; Zhang, C. Green synthesis of silver nanoparticles using *Chenopodium aristatum* L. stem extract and their catalytic/antibacterial activities. *J. Clust. Sci.* **2017**, *28*, 1319–1333. [[CrossRef](#)]
39. Iravani, S.; Zolfaghari, B. Green synthesis of silver nanoparticles using *Pinus eldarica* bark extract. *BioMed Res. Int.* **2013**, 639725.
40. Cruz, D.; Falé, P.L.; Mourato, A.; Vaz, P.D.; Luisa Serralheiro, M.; Lino, A.R.L. Preparation and physicochemical characterization of Ag nanoparticles biosynthesized by *Lippia citriodora* (Lemon Verbena). *Colloid Surf. B Biointerfaces* **2010**, *81*, 67–73. [[CrossRef](#)] [[PubMed](#)]



© 2019 by the authors. Licensee MDPI, Basel, Switzerland. This article is an open access article distributed under the terms and conditions of the Creative Commons Attribution (CC BY) license (<http://creativecommons.org/licenses/by/4.0/>).